Thin-Layer Drying Models and Artificial Neural Network for Wood Fiber in a Near-Infrared Dryer

Mohammad Arabi ,* and Mohammad Dahmardeh Ghalehno

The purpose of this study was to fit and compare semi-empirical thin-layer drying models and an artificial neural network (ANN) model to describe the drying kinetics of wood fiber in a near-infrared (NIR) dryer. The drying kinetics of wood fiber were evaluated using 18 semi-empirical models at three temperatures (105, 120, and 135 °C), utilizing a halogen moisture analyzer. The ANN model was designed with temperature and time as input factors and moisture content as the output variable. The findings revealed that the drying process was mainly controlled by a diffusion mechanism, and all the process occurred in two falling drying rate periods. The fitness of drying curves on semi-theoretical models based on statistical parameters, including RMSE, SSE, and R^2 showed that there was not much difference between equations with a maximum of two constant parameters and equations with more than two constant parameters. Therefore, using a simple model can help to reduce the time of the analysis and is beneficial to avoid using complex drying models. Also, the results showed that at higher drying temperatures (120 to 135 °C), both ANN and the best-performing semi-empirical models (Page and Henderson–Pabis) produced comparable accuracy, whereas at lower temperature (105 °C), ANN performed better due to its flexibility.

DOI: 10.15376/biores.21.1.654-672

Keywords: Artificial neural network; Drying kinetics; Moisture content; Wood fiber

*Contact information: Department of Wood Science and Technology, Faculty of Natural Resources, University of Zabol, Zabol, Iran; * Corresponding author: marabi@uoz.ac.ir*

INTRODUCTION

During drying, hornification occurs within the cell wall, where pore structures tend to shrink and partially close as moisture is removed. This phenomenon reduces the accessibility of bound water and alters diffusion dynamics (Sjöstrand *et al.* 2023). As a result, researchers and industry owners have considered strategies to recognize and manage the drying process of wood and cellulose fiber. Modeling the drying process of cellulose fiber is one technique to identify and manage the drying process. Several investigations have been carried out to simulate and examine the drying kinetic of wood and cellulosic fibers based on Fick's law of diffusion (Dincer 1998; Wang *et al*. 2007a; Remond *et al*. 2005; Salin 2008; Fernando *et al*. 2018; Autengruber *et al*. 2020; Chanpet *et al*. 2020). Recently, several studies have shown that the theoretical models do not adequately describe the fundamental aspects of the experimental wood drying process. Remond *et al*. (2005) indicated that when softwoods dry, a thin and dry shell without free water develops quickly in the substrate near the wood surface, slowing the drying process and releasing free water from the substrates. These substrates are still saturated with free water. It has been shown by Wiberg and Moren (1999) that at the beginning of the drying process with high moisture

content, the moisture in the central part of sapwood decreases very rapidly without any moisture gradients. The diffusion phenomenon cannot describe the moisture migration process gradient-free.

Also, dynamic changes in the pore size of wood cell wall occur during drying process. So, when surface moisture evaporates quickly, the surface of the fibers also dries quickly, resulting in the highest wood shrinkage. Moreover, the diameter of pores in the wood cell wall will be decreased. Consequently, moisture cannot be transferred from the lower layers near the surface to the fiber's surface (Li and Zhao 2020). Some researchers believe that some of the interactions and relationships between water and wood during the drying process at the microstructural scale are still unknown (Penttila *et al*. 2021; Zitting *et al*. 2021). As a result, mathematical modeling of the drying process of wood and cellulose fiber seems to be complex (Sander *et al*. 2010). Due to shrinkage and deformation in the cell walls of wood fibers during the drying process, the accuracy of the presented mathematical models is questioned.

The drying process of lignocellulosic materials, agricultural products, and food has been modeled using various semi-empirical and experimental models (Verma *et al.* 1985; Babalis *et al.* 2006; Demir *et al.* 2007; Doymaz 2007; Gan and Pe 2014). These models are typically not mechanistically derived mathematical models; instead, they are formulated using simplified analytical expressions that are fitted to experimental data. Fick's second law and its variants, as well as Newton's law of cooling, are often used as a basis for constructing such semi-empirical relations. Because these models are developed directly from laboratory observations, they are generally less complex and more accessible than fully mechanistic mathematical models (Wang and Singh 1978; Hii et al. 2009; Kumar et al. 2012). Also, these empirical models have shown a strong capacity to estimate and forecast the drying kinetics of various materials (Ertekin and Firat 2017; Midili *et al*. 2002). Modeling the thin-layer drying of materials is mainly based on describing the moisture ratio (MR) *versus* time (*t*) data by using suitable mathematical model or models (Ademiluyi *et al*. 2008; Kaleta *et al*. 2013). Thin-layer drying means to dry as one layer of sample particles or slices. It is assumed that there is the same air velocity and temperature throughout this thin layer (Vega *et al*. 2007; Lee and Kim 2009; Kaur and Singh 2014). The drying kinetics of bacterial cellulose (Jatmiko *et al*. 2017), cotton fibers (Ghazanfari *et al*. 2006), and unbleached kraft pulp sheets (Kong *et al*. 2022) have all been investigated using thin-layer drying models, with promising findings.

The use of artificial neural networks (ANNs) is one of the newest techniques for modeling and forecasting complex dynamic systems such as the wood drying process. Some researchers have utilized the ANNs to simulate the drying process of wood and agricultural products (Chai *et al*. 2018; Dash *et al*. 2020; Saxena *et al*. 2022). The neural network models have been utilized to simulate agricultural product drying kinetics as well as the wood drying process. Previous research has shown that the ANN model is more advantageous, since it can precisely predict the drying kinetics and be easily applicable to non-linear processes (Saxena *et al*. 2022). Former studies have employed conventional and convective dryers to determine the drying kinetics of wood particles and cellulose fibers (Zarea Hosseinabadi *et al*. 2012; Górnicki *et al*. 2016; Arabi *et al*. 2017; Brys *et al*. 2021; Kong *et al*. 2022). These drying methods have several drawbacks, including low energy efficiency and lengthy drying time, especially in falling drying rate periods (Wang *et al*. 2007). Radiant dryers, such as halogens lamps, deliver heat to the material more quickly than convective or conductive dryers. As a result, the drying time decreases. The halogen hygrometer is one of the latest quick and precise methods for detecting the moisture content

of various materials. Halogen hygrometers are now acknowledged as a scientific, accurate approach and ASTM-accepted method in the industry (ASTM D6980-12). This is the first study to use a halogen hygrometer to describe the drying kinetics of wood fiber analysis.

There are now more than more than 100 different semi-theoretical and empirical thin-layer drying models that have been used in predicting moisture content of agricultural products (Ertekin and Firat 2017). Each of the models is composed of dimensionless constants (a, b, c, d, and…) and drying constants (k, g, K_1, K_2, and K_0). Increasing the numbers of parameters helps researchers to better analysis and predicts the dependent variable, but this is also a tedious and time-consuming task. Therefore, in this study, about 18 thin layer drying models with different numbers of fixed parameters and an ANN model were investigated to select the simplest possible model as the best model for prediction of wood fiber drying data.

EXPERIMENTAL

Wood fibers (A mixture of forest and garden species) were obtained from the Arian Sina factory (MDF Production). In order to investigate the drying rate of wood fibers above FSP, they were combined with water in equal weight ratios for 24 h and then stored in a sealed polyethylene bag at 3 °C to 5 °C for seven days. The sample was mixed every day to ensure that the wood fibers had a consistent moisture level. Finally, wood fiber with a moisture content of 170% (based on dry weight) was subjected to the drying process.

Fig. 1. Moisture analyzer, MB45 AM (ohaus.com)

Drying Process

A moisture analyzer Halogen model MB45, manufactured by OHAUS, was used to dry wood fibers at three different temperatures: 105, 120, and 135 °C (Fig. 1). The MB45 has a sample capacity of 45 g, with a readability of 0.001 g and repeatability of 0.015% (using a 10 g sample). The heater type of MB45 is a halogen lamp, and the operating temperature range is 50 to 200 °C in 1 °C increments.

In halogen hygrometers, the sample is heated by absorbing the infrared (IR) radiation produced by the halogen lamp. The weight difference before and after dryings is used to determine the mass and moisture content of the sample continuously throughout the drying process. Halogen hygrometers work on the Loss on Drying (LOD) principle, as in the case of oven dryers. However, there are various benefits such as quick drying time, ease of use, and direct measurement without computations compared to the oven dryer.

To investigate the drying kinetics of wood fibers, 4 g of wet fibers were dispersed on a stainless-steel tray placed on a precise and sensitive scale in the dryer compartment. The fiber was distributed on a tray carefully to prevent the fibers from accumulating at single points. After adjusting the temperature of the dryer chamber in the scope of this study, the weight loss values of the samples at a specified time interval, every 30 s, were presented and recorded online on the hygrometer display. The wood fibers continued to dry until the sample's moisture content was nearly zero. The tests were performed three times for each temperature, and the mean moisture content measurements were used to design and fit the drying curves for each temperature.

Drying Kinetics of Wood Fibers

The moisture content of wood fibers was measured according to Eqs. 1 and 2,

$$\mathrm{MR} = \left(\frac{M_{\mathrm{t}} - M_{\mathrm{e}}}{M_0 - M_{\mathrm{e}}}\right) \quad (1)$$

$$\mathrm{MR} = \left(\frac{M_{\mathrm{t+dt}}}{M_0}\right) \quad (2)$$

where MR is the moisture ratio (dimensionless), M_t is the moisture content at time t (kg of solids/kg of water), M_e is the equilibrium moisture (kg of solids/kg of water), and M_0 is the initial moisture content (kg of solids/kg of water).

It should be noted that due to the insignificant value of M_e in comparison with Mt and M_0, it can be ignored. Therefore Eq. 1 can be simplified to Eq. 2. (Doymaz 2007; Ertekin and Firat 2017).

The drying rate of wood fibers was measured using Eq. 3 (Ertekin and Firat 2017),

$$\mathrm{DR} = \left(\frac{M_{\mathrm{t+dt}} - M_{\mathrm{t}}}{\mathrm{dt}}\right) \quad (3)$$

where M_t and M_{t+dt} are the MC values at t and $t+dt$ (kg moisture/kg dry matter), respectively, and t is drying time (s). Equation 2 was used to obtain the MR of wood fibers at each temperature. Then, the experimental drying data of MR *versus* time was fitted to thin drying layer models using MATLAB 2016 software. The models listed in Table 1 have already been widely used to investigate the drying kinetics of food, agricultural products, and municipal waste.

The performance of these models was examined by comparing the coefficient of determination (R^2), sum squares of error (SSE), and root mean squared error (RMSE)

which were calculated in Eqs. 4 to 6, respectively. The best thin drying layer model is the one with the smallest error value and the greatest coefficient of determination,

$$R^2 = \frac{\sum_{i=1}^{N}(MR_{\exp,i} - \overline{MR}_{\exp})(MR_{pre,i} - \overline{MR}_{pre})}{\sqrt{\left[\sum_{i=1}^{N}(MR_{\exp,i} - \overline{MR}_{\exp})^2\right]\left[\sum(MR_{pre,i} - \overline{MR}_{pre})^2\right]}} \quad (4)$$

$$\mathrm{RMSE} = \left[\frac{1}{\mathrm{N}}\sum_{\mathrm{I}=1}^{\mathrm{n}}(\mathrm{M}_{\mathrm{pre,i}} - \mathrm{M}_{\mathrm{exp,i}})\right]^{1/2} \quad (5)$$

$$\mathrm{SSE} = \sum_{\mathrm{i}=1}^{\mathrm{n}}(MR_{\mathrm{pre,i}} - MR_{\mathrm{exp}})^2 \quad (6)$$

where MR_{prei} and MR_{expi} are the predicted and experimental moisture ratio values at i_{th} observation, respectively. The MR_{exp} is the mean value of the explanatory variable, N is the number of observations, and n is the number of model parameters.

Table 1. Mathematical Models Applied to Drying Curves

Model Name	Model Equation	Parameters	Reference
Lewis (Newton)	MR = exp(−*kt*)	*k*	Ghazanfari *et al.* 2006
Henderson and Pabis	MR = *a* exp(−*kt*)	*a*, *k*	Kaur and Singh 2014
Logarithmic	MR = *a* exp(−*kt*) + *c*	*a*, *k* , *c*	Gan and Poh 2104
Modified Midilli *et al*.-III	MR = *a* exp(−*kt*) + *ct*	*a*, *k*, *c*	Kaur and Singh 2014
Two-term	MR = *a* exp(−k_1 *t*) + *c* exp(−k_2 *t*)	*a*, k_1, k_2, *c*	Kumar *et al*. 2014
Noomhorm and Verma	MR = *a* exp(−k_1 t) + b exp(−k_2 t) + c	*a*, *b*, *c*, k_1, k_2	Kaleta and Gornicki 2010
Modified Henderson and Pabis	MR = *a* exp (−k_1 *t*) + *b* exp(−k_2 *t*) + *c* exp(−k_3 *t*)	*a*,*b*,*c*,k_1,k_2,k_3	Erbay and Icier 2009
Two-term exponential	MR = *a* exp(−k_1*t*) + (1 − *a*) exp(−*a*k_2*t*)	*a*,k_1,k_2	Lee and Kim 2009
Modified two term-V	MR = *a* exp(−*kt*) + (1 − *a*) exp(−*gt*)	*a*, *g*, *k*	Verma *et al*. 1985
Page	MR = exp (−kt^n)	*k*, *n*	Doymaz 2007
Modified Page-IV	MR = *a* exp(−kt^n)	*a*, *k*, *n*	Babalis *et al*. 2006
Hii *et al*.	MR = *a* exp (−kt^n) + *c* exp(−gt^n)	*a*, *k*, *n*, *c*, *g*	Hii *et al*. 2009
Kaleta *et al*. II	MR = *a* exp(−kt^n) + (1 − *a*)exp(−gt^n)	*a*, *k*, *n*, *g*	Kaleta *et al*. 2013
Modified Page II	MR = exp[−(*kt*)^n]	*k*, *n*	Vega *et al*. 2007
Modified page .III	MR = *a* exp[−(*kt*)^n]	*a*, *k*, *n*	Ertekin and Firat 2017
Demir *et al*.	MR = *a* exp[−(*kt*)^n] + *c*	*a*, *k*, *c*, *n*	Demir *et al*. 2007
Wang and Singh	MR = 1 + *at* + kt^2	*a*, *k*	Wang and Singh 1978
Midilli *et al*.	MR = *a* exp(−kt^n) + *ct*	*a*, *k*, *n*, *c*	Midilli *et al*. 2002

Artificial Neural Network Model

An artificial neural network (ANN) is a nonlinear modeling method. It is generally used to model complex physical phenomena such as the drying process of wood and lignocellulosic materials. The ANN configuration used in this study was a Multi-layer perceptron (MLP). A MLP is a feed forward ANN model that generates a set of outputs from a set of inputs. The MLP is characterized by several layers of input nodes connected as a directed graph between the input and output layers. The MLP uses backpropagation for training the network and it consists of three types of layers-the input layer, output layer, and hidden layer, as shown in Fig. 2.

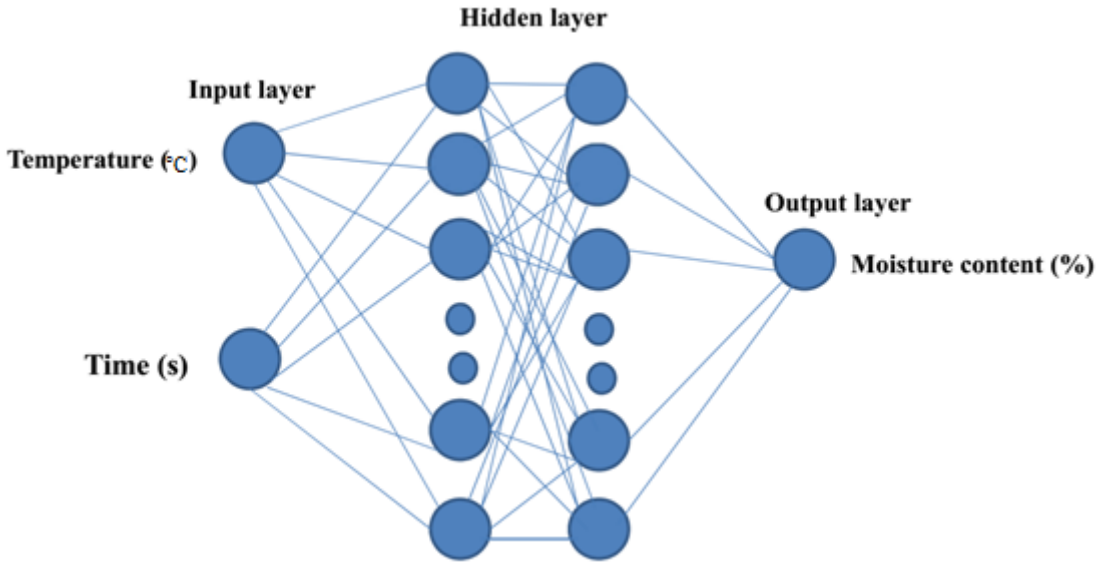

Fig. 2. Scheme of artificial neural network for prediction moisture content of wood fiber

The data employed for experimental study were randomly divided into three groups: 70% in the training set, 15% in the validation set, and 15% in the test set. The structure of the three-layer feed-forward network studied in this paper was built using two input variables (temperature and drying time) and one the outputs variables (moisture content). Different number of neurons in the hidden layer was applied based on the trial method to develop the optimum ANN model that can minimize the deviations between the predicted and experimental results. The neural network was trained using the Levenberg-Marquardt (LM) learning algorithm. The hyperbolic tangent sigmoid transfer function was as follows,

$$f(x) = \frac{2}{1 + e^{(-2x)}} - 1 \quad (7)$$

where $f(x)$ and x are the output and input values of neurons, respectively.

The coefficient of determination (R^2), mean squared error (MSE), and mean absolute error (MAE) were used to predict the ANN performance. Equations 8 to 10 include the formulas for computing these statistical characteristics,

$$MAE = \frac{1}{n}\sum_{i=1}^{n}\left(\frac{|y_{exp.} - y_{pred.}|}{y_{exp.}}\right)100 \quad (8)$$

$$MSE = \frac{1}{n}\sum_{i=1}^{n}\left(y_{exp.} - y_{pred.}\right)^2 \quad (9)$$

$$R^2 = 1 - \frac{\sum_{i=1}^{n}\left(y_{exp.} - y_{pred.}\right)^2}{\sum_{i=1}^{n}\left(y_{exp.} - \overline{y_{exp.}}\right)^2} \quad (10)$$

where y_{exp} is the actual data value, y_{pred} is the predicted data value, y_{pred} with a line above it is the average of the actual values, and n is the number of data.

RESULTS AND DISCUSSION

Drying Curves

Figure 3 depicts the drying behavior of wood fiber using a moisture analyzer at 105, 120, and 130 °C. Accordingly, reaching the target moisture content from 170% (based on dry weight) to final moisture content (near zero) took 18, 14, and 12 min for 105, 120, and 135 °C, respectively. As shown in Fig. 3, the increase in the drying temperatures significantly decreased the drying times.

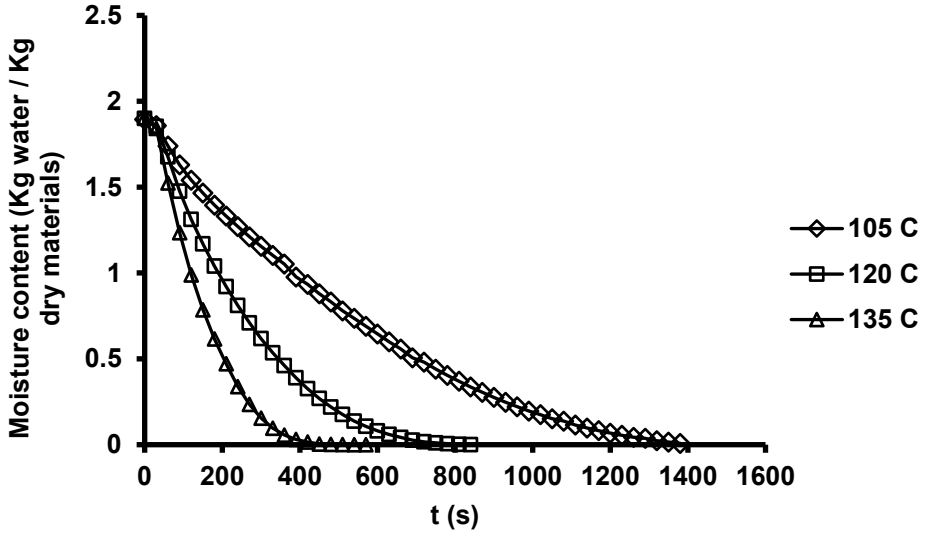

Fig. 3. Moisture content versus drying time at different halogen drying temperature

In the Ohaus halogen moisture analyzer MB Series, the halogen radiator emits infrared radiation (IR) in the short wavelength range of 0.75 to 1.5 µm (near-infrared). When the halogen lamp is radiated toward the product, it is strongly heated and the thermal gradient within the material significantly increases in a short period. Since the halogen radiant energy easily passes through air without heating the ambient air, this energy just heats the product. Thus, the internal part of the materials will be warmer than the surrounding air and the rate of heat transfer will be greater as compared to the hot air-drying technique (Younis *et al*. 2018; Huang *et al*. 2021). Therefore, IR drying technology has the advantages of high energy efficiency, short drying time, uniform heating of materials, and low energy costs (Huang *et al*. 2021).

The changes in drying rates *versus* drying time are shown in Fig. 4. Accordingly, the drying rate increased with an increase in drying temperature. Also, the drying speed was quick at the beginning of the drying operation (especially at a higher temperature), but the drying rate was slowed with passing time. This is due to a lack of sufficient moisture at the end point of the drying process.

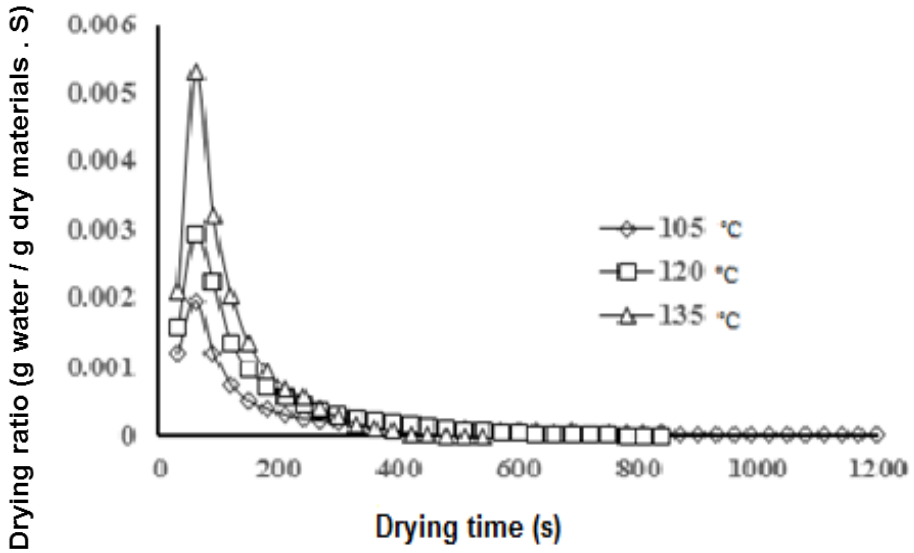

Fig. 4. Drying rate versus drying time at different halogen drying temperature

The relationship between drying rate and moisture content at different drying temperatures is shown in Fig. 5. The three drying periods were observed, including a preheating period (A) and the first and second drying rate periods (B and C). A constant drying rate was not found; however, the initial moisture content of wood fibers was about 170% (based on dry weight). The morphological structure of fibers and drying techniques can significantly affect the drying process. When wood fibers are heated quickly by the moisture analyzer, many morphological changes might occur in their structures. The microstructure and rheological behavior of the wood cell wall are closely intertwined with its moisture properties. External layers of wood fibers shrink rapidly. First, a thin and dry shell are formed near the surface of fibers, which creates barriers for migration of moisture from internal layers to the surface (Li and Zhao 2020). Due to these morphological interactions, even if there is a lot of free water in the bottom layers, the rate of migration of water molecules from the interior to the surface is less than the rate of vaporization from the surface into the environment. Therefore, it is extremely difficult to find a constant drying rate period during the drying process of wood fibers. For lignocellulosic materials, constant drying rate periods are often extremely short or not seen at all (Zarea Hosseinabadi *et al*. 2012; Arabi *et al*. 2017; Kong *et al*. 2020). The heat and mass transfer in the drying process of a solid material can be defined based on the Biot number (*Bi*), which is a dimensionless number that represents the ratio of the resistance to heat transfer from the inside of the body to the surface (Sander *et al*. 2010). Constant drying is observed for solid materials with a Bi number less than 0.1, while the *Bi* number value for lignocellulosic materials was reported as more than 0.2 . It means that the drying process and mass transfer parameters for biomass materials were mostly controlled by internal resistance (Dincer

1998). According to Fig. 5, the drying process almost completely occurred during the first and second falling rate periods (B and C).

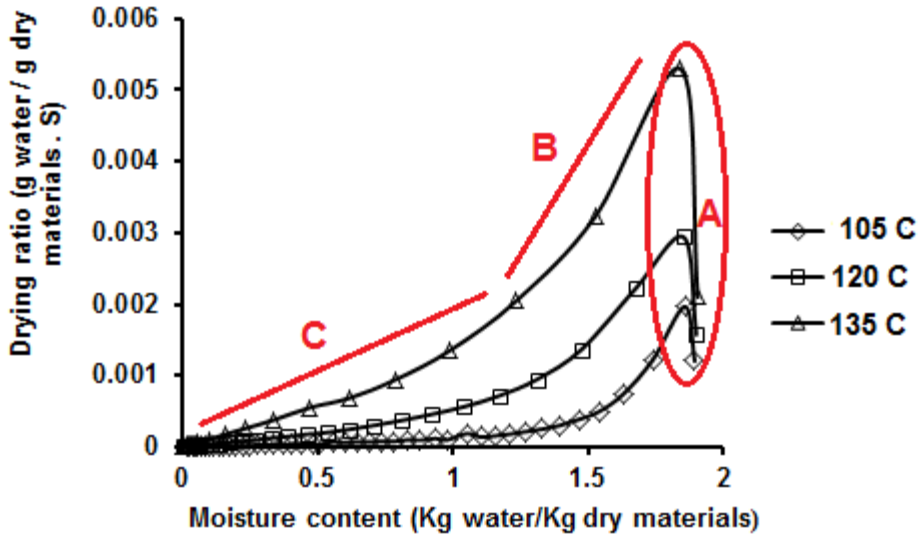

Fig. 5. Drying rate *versus* moisture content at different halogen drying temperature

The first falling drying rate happened when wet spots on the surface gradually diminished until the whole surface was dry. As a result, the surface moisture of the fibers decreased over time while the surface temperature increased. During this period, the drying process was controlled by moisture diffusion and internal resistances inside wood fibers. When the surface was totally dried, the second falling drying rate started at point C, and the dry surface was transmitted to the layers underneath the surface. According to Fig 5, about 60% of the total drying time occurred during this period. In this phase, the drying rate was independent of drying conditions such as temperature and moisture content. The moisture transfer might be due to liquid diffusion, capillary movement, and vapor diffusion. Also, the drying time was usually greater than the first falling drying rate period.

Drying Curves Fitting

The nonlinear regression approach and MATLAB 2016 software were used to fit moisture content data at various drying temperatures to the thin-layer drying models presented in Table 1. The regression constants (a, b, c, d...,), the drying constants (k), and the statistical indicators (R^2, SSE, and RMSE) of the thin-layer drying models are shown in Tables 2, 3, and 4 for 105, 120, and 135 °C, respectively.

According to Tables 2, 3, and 4, Lewis model (Newton) with the one fixed parameter (k), Wang and Singh and Modified Page-II models with two constant parameters, and Two-term exponential models with three constant parameters did not show a good fitness for moisture content prediction. At 105 °C, the Lewis model exhibited poor fitting (R^2 = 0.522) due to high internal resistance and non-uniform moisture distribution. However, at higher temperatures (120 and 135 °C), diffusion resistance decreased, and the drying process became more surface-controlled, resulting in more exponential behavior and improved model fitting, as evidenced by higher R^2 values.

Table 2. Statistical Results and Drying Constant of Mathematical Models at Different Drying Temperature (T = 105 ºC)

T	Model	adj. R^2	Constant Parameters	RSME	SSE
105	$F(t) = \exp(-kt)$	0.3308	k = 0.001095	0.3785	17.91
	$F(t) = a\exp(-kt)$	0.9804	a = 2.004, k = 0.002016	0.06489	0.5221
	$F(t) = a\exp(-kt) + c$	0.9987	a = 2.352, k = 0.00129, c = -0.4487	0.01638	0.03298
	$F(t) = a\exp(-kt) + c\,t$	0.9986	a = 1.909, k = 0.001517, c = -0.0002181	0.01715	0.03619
	$F(t) = a\exp(-k_1t) + c\exp(-k_2t)$	0.9987	a = 58.78, k_1 = 0.0007727, k_2 = 0.0007472, c = -56.89	0.01646	0.03304
	$F(t) = a\exp(-k_1t) + b\exp(-k_2t) + c$	0.9987	a = 2.361, k_1 = 0.00126, k_2 = 0.01683, b = 0.02563, c = -0.471	0.01627	0.03205
	$F(t) = a\exp(-k_1t) + b\exp(-k_2t) + c\exp(-k_3t)$	0.9973	a = 20.62, k_1 = 0.0002808, k_1 = 0.003502, k_3 = 0.0002256 b = 0.5778, c =-19.28	0.02422	0.07037
	$F(t) = a\exp(-k_1t) + (1-a)\exp(-ak_2t)$	0.3837	a =18.57, k_4 = 0.0003812, k_2 =1.902e-05	0.3655	16.43
	$F(t) = a\exp(-kt) + (1-a)\exp(-gt)$	0.8920	a = 2.035, k = 0.002048, g = 0.9649	0.153	2.878
	$F(t) = \exp(-kt^n)$	0.9874	k= 2.326e-08, n = 2.617	0.05198	0.335
	$F(t) = a\exp(-kt^n)$	0.9937	a =1.827, k = 0.0002737, n = 1.298	0.03695	0.1679
	$F(t) = a\exp(-kt^n) + (1-a)\exp(-gt^n)$	0.9043	a = 1.787, k = 0.0001936, g = 0.9649, n = 1.348	0.1445	2.548
	$F(t) = a\exp(-kt^n) + bt$	0.9990	a = 1.571, k = 7.104, c = -0.001415, n = -9.327	0.02559	0.02934
	$F(t) = 1+at+kt^2$	0.5641	a = 0.00017, k = -9.287e-07	0.3061	11.62
	$F(t) = a\exp[-(kt)^n]$	0.9937	a =1.827, k = 0.001797, n =1.298	0.03695	0.1679
	$F(t) = \exp[-(kt)^n]$	0.5989	k = 0.001215, n = 3.284	0.2925	10.61
	$F(t) = a\exp[-(kt)^n] + c$	0.9987	a = 2.359, k = 0.001285, c = -0.4543, n = 0.9974	0.02644	0.03298

Henderson and Pabis and Page models with two adjustment parameters and Logarithmic, Modified Midilli *et al*.-III, Modified Page-III and Modified Page-IV models with three adjustment parameters showed good fits for the wood fiber drying process. Also, Demir *et al*., Midilli *et al*., Hii *et al*., Kaleta *et al*. II., Two-term, Noomhorm and Verma, Modified Henderson and Pabis model with more than three adjustment parameters predicted moisture content of wood fiber with the highest value of R^2 and lowest value of RMSE and SSE.

According to results of Tables 2, 3, and 4, based on the statistical indicators; there was not much difference among some of models with two, three, and more than three adjustment parameters. The Midilli *et al*. model with four fixed parameters were selected as a best model for drying kinetic of wood poplar particle (Zarea Hosseinabadi *et al*. 2012; Arabi *et al*. 2017).

Table 3. Statistical Results and Drying Constant of Mathematical Models at Different Drying Temperature (T=120 °C)

T	Model Equation	adj. R^2	Constants	RSME	SSE
120 °C	$f(t) = \exp(-kt)$	0.98334	k = 0.003745	0.06306	0.09942
	$f(t) = a \exp(-kt)$	0.9986	a = 2.116, k = 0.00577	0.01889	0.008567
	$f(t) = a \exp(-kt) + c$	0.99762	a =2.145, k_1 =0.002314, c = -0.06061	0.02282	0.0198
	$f(t) = a \exp(-k_1 t) + c \exp(-k_2 t)$	0.9965	a = 2.157, k_1 = 0.005964, k_2 = 0.9134, c = -0.2919	0.03085	0.02094
	$f(t) = a \exp(-k_1 t) + b \exp(-k_2 t) + c$	0.9993	a = 2.155, k_1 = 0.005375, k_2 = 0.9134, b = -0.2292, c = -0.06012	0.02445	0.004384
	$f(t) = a \exp(-k_1 t) + c \exp(-k_2 t) + b \exp(-k_3 t)$	0.9965	a = 2.158, k_1 = 0.005965, k_2 = 0.9134, k_3 = 0.2735, b = -0.402, c = 0.1097	0.03236	0.02094
	$f(t) = a \exp(-kt) + (1-a) \exp(-ak_1 t)$	0.96682	a = 2.134, k = 0.00585, k_1 = 0.9134	0.09278	0.198
	$f(t) = a \exp(-kt) + (1-a) \exp(-gt)$	0.96682	a =2.134, k = 0.00585, g = 0.9134	0.09278	0.198
	$f(x) = a \exp(-kt^n)$	0.99734	a = 1.898, k = 0.001704, n = 1.208	0.02652	0.01617
	$f(x) = \exp(-kt^n)$	0.57398	k = 1.629e-08, n = 2.979	0.3207	6.581
	$f(t) = a \exp(-kt^n) + (1-a) \exp(-gt^n)$	0.95142	a =1.954, k = .002078, g = 1.403, n = 1.178	0.1148	0.29
	$f(t) = a \exp(-k\, t^n) + c \exp(-g\, t^n)$	0.9993	a =1.125, k=2.499e-05, c = 0.7501, g = 0.00024, n = 1.87	0.007601	0.001213
	$f(t) = a \exp(-kt^n) + ct$	0.99776	a = 1.907, k = 0.002072, c = -3.828e-05, n = 1.168	0.02442	0.01311
	$f(t) = 1+at+kt^2$	0.6171	a = -0.002029, k = 7.124e-07	0.3084	2.282
	$f(t) = a \exp[-(kt)^n]$	0.99734	a =1.898, k = 0.0051, n = 1.208	o.02652	0.01617
	$f(t) = \exp[-(kt)^n]$	0.9608	k = 0.003214, n = 2.116	0.9868	0.2337
	$f(t) = a \exp[-(kt)^n] + c$	0.99776	a =1.937, k = 0.00498, c = -0.02897, n = 1.16	0.02445	0.01316

Additionally, Kong *et al.* (2020) presented a complex model (the Yun model) with five fixed parameters for predicting the drying kinetics of pulpboard, achieving very high accuracy (Adjusted R^2 = 0.999; RMSE = 0.003). The drying behavior of sawdust mixtures has also been investigated by Górnicki *et al.* (2016), who reported that the Logarithmic, Noomhorm, Verma (Kaleta and Gornicki 2010), Demir *et al.* (2007), and Midilli *et al.* (2002) models showed the best performance when fitting experimental data. However, Buzrul (2022) emphasized that in complex models—particularly those with more than two parameters—some parameters may be statistically non-significant ($p > 0.05$), and therefore the use of unnecessarily complex models may not be justified.

In the present study, the Adjusted R^2 and RMSE values for the Henderson and Pabis and Page models, each containing a maximum of two fixed parameters, ranged from 0.9785 to 0.9832 and from 0.0998 to 0.0824, respectively. These Adjusted R^2 values, which account for the number of model parameters, confirm that increasing model complexity does not lead to a meaningful improvement in predictive performance. Therefore, it can be concluded that the Henderson and Pabis and Page models, as simple and statistically efficient models, are the most appropriate choices for describing the thin-layer drying process of wood fibers.

Table 4. Statistical Results and Drying Constants of Mathematical Models at Different Drying Temperature (T = 135 °C)

T	Model	adj. R^2	Constants	RSME	SSE
135 °C	$f(t) = \exp(-kt)$	0.9797	k = 0.006706	0.07281	0.1007
	$f(t) = a\exp(-kt)$	0.99678	a = 2.366, b = 0.01029	0.02914	0.01528
	$f(t) = a\exp(-kt) + c$	0.98404	a = 2.083, b = 0.008413, c = -0.05057	0.06703	0.07638
	$f(t) = a\exp(-k_1t) + c\exp(-k_2t)$	0.99916	a = 2.411, k = 0.01053, k_1 = 0.975, c =-0.5302	0.01536	0.003775
	$f(t) = a\exp(-k_1t) + c\exp(-k_2t) + d$	0.9993	a = 2.402, k = 0.01029, k_1 = 0.975, c = -0.5089, d = -0.01262	0.001748	0.002727
	$f(t) = a\exp(-k_1t) + c\exp(-k_2t) + d\exp(-k_3t)$	0.99916	a = 2.411, k_1 = 0.01054, k_2 = 0.975, k_3 = 0.5469, c = -0.2046, d = -0.3261	0.01642	0.003775
	$f(t) = a\exp(-k_1t) + (1-a)\exp(-ak_2t)$	0.83788	a = 2.411, k_1 = 0.01054, k_2 = 0.975	0.2141	0.7795
	$f(t) = a\exp(-kt) + (1-a)\exp(-gt)$	0.8376	a = 2.411, k = 0.01054, g = 0.9649	0.2141	0.7795
	$f(t) = a\exp(-kt^n)$	0.9958	a = 1.932, k = 0.001844, n = 1.312	0.03431	0.02001
	$f(t) = \exp(-kt^n)$	0.68836	k = 6.524e-07, n = 2.718	0.2882	1.495
	$f(t) = a\exp(-kt^n) + (1-a)\exp(-gt^n)$	0.83774	a = 2.288, k = 0.007153, g = 0.9649, n = 1.07	0.2206	0.7784
	$f(t) = a\exp(-kt^n) + c\exp(-gt^n)$	0.9993	a = 2.288, k = 0.007151, g = 0.975, c = -0.4077, n =1.07	0.001326	0.001638
	$f(t) = a\exp(-kt^n) + ct$	0.96766	a = 0.02299, b = -0.001318, k =-5.648, c = -0.06798	0.09136	0.1753
	$f(t) = 1+at+kt^2$	0.93434	a = -0.004318, k = 4.627e-06	0.1323	0.3149
	$f(t) = a\exp[-(kt)^n]$	0.9958	a = 1.932, k = 0.008252, n = 1.312	0.03431	0.02001
	$f(t) = \exp[-(kt)^n]$	0.6885	k = 0.005315, n = 2.791	0.2882	1.495
	$f(x) = a\exp[-(kt)^n] + c$	0.99608	a = 1.913, k = 0.008354, c = 0.01465, n = 1.344	0.03409	0.0186

ANN Model

A multilayer perceptron consisting of layers with one or more neurons with different activation functions was employed to optimize the perceptron network. The MLP model was developed based on temperature and drying time as input variables and moisture content as an output variable. The number of neurons in the hidden layer is the variable (x). Experimental data were separated into three groups for the ANN modeling, including training (70%), validation (15%), and testing (15%). After training and testing the network, the findings revealed that topology 2-5-1 with hyperbolic tangent sigmoid transfer functions provided the greatest training for moisture modeling. The R values for MR for neural network training, validation, and testing data are shown in Fig. 6. In the training, validation, and testing data, as well as the total data, the R-values for MR were 0.99956, 0.99979, 0.99947, and 0.99958, respectively.

According to Table 5, the total data in the ANN model for MR prediction had an absolute mean percent error (MAPE) of 2.53%. The ANN showed a higher capacity to predict the moisture content of wood fibers than regression and thin-layer drying models, as evidenced by the high coefficient of determination and low error percentage between experimental and predicted data.

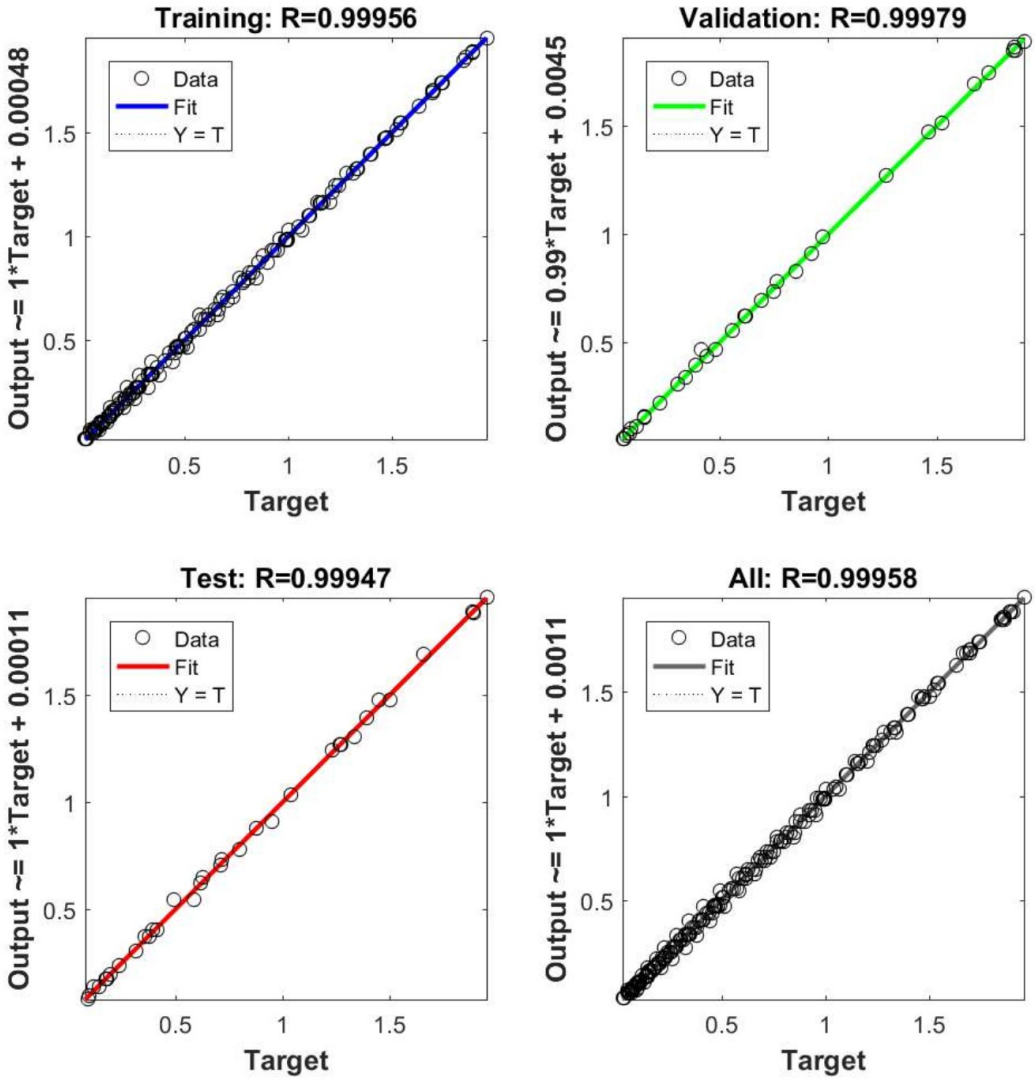

Fig. 6. Regression plots of the developed ANN model for (a) the training data set, (b) the validation data set, (c) the testing data set, and (d) all data

Table 5. Evaluation of the Performance of ANN using Statistical Parameters

Factor	Parameter	R	MSE	MAPE	
	Training	0.99998	**0.000011**		
MC	Validation	0.99998	**0.000014**		
	Testing	0.99993	**0.00005**		
	All Data	**0.99997**		2.53	

Figure 7 depicts experimental data against predicted data obtained based on ANN models. Accordingly, the neural network predicted the experimental data (R^2) more accurately than Midilli *et al*. (2002) model. Artificial neural networks are unique machine learning algorithms that mimic the human brain and find the relationship between the data sets. Therefore, ANN can learn from the past data and improve its performance based on previous experience and training. Moreover, the designed program can adapt to new

conditions in case of data change. These two factors of generalizability and adaptability distinguish the ANN from other modeling methods and allow it to provide better results than other modeling methods. Many researchers have utilized ANNs to predict the drying process of wood and lignocellulosic materials. These studies employed MAPE, MSE, and R^2 statistical parameters as the main comparison between experimental and predicted data.

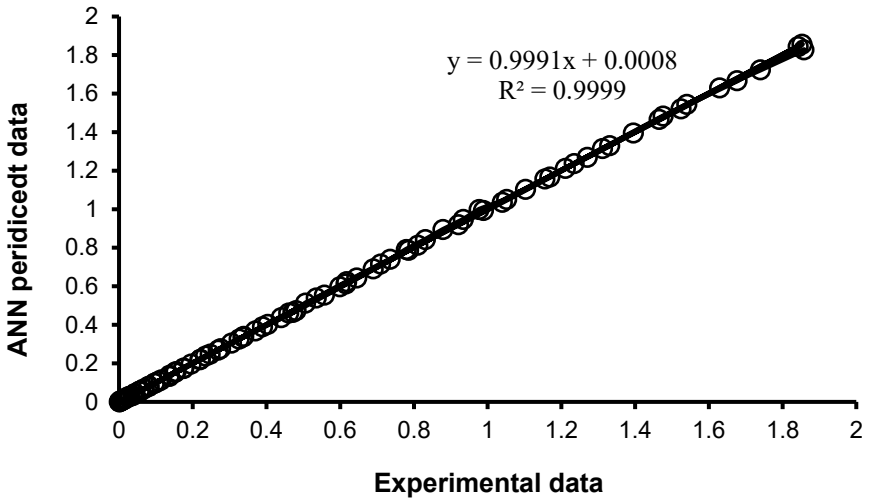

Fig. 7. Comparison of ANN predictions and experimental data

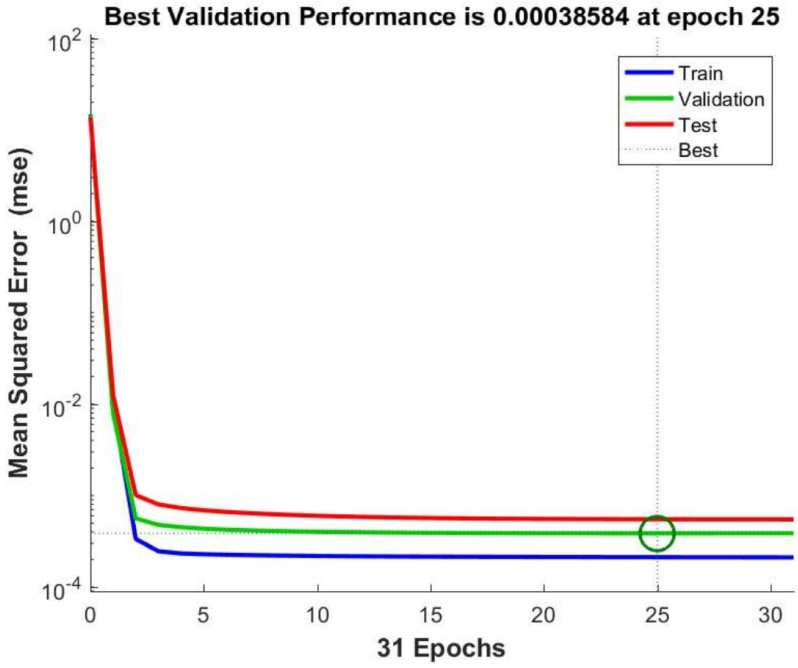

Fig. 8. Neural network performance by period (epoch) for training, validation, and testing data

The findings from the current study are consistent with results from previous studies (Saxena *et al*. 2022). Overfitting is the most common issue in neural network training. This issue occurs when a neural network only performs well on training data and does not provide good results for other data sets. A periodic epoch performance chart for a neural network is shown in Fig. 8, when the error due to the validation data stays constant for six consecutive epochs, the neural network computation stops.

As shown in Fig. 8, after 25 epochs, the error was fixed in the following six consecutive periods, and the forecasting and data processing was stopped. This showed the network has been well-trained, validated, and tested.

Sensitivity Analysis of ANN Model

A sensitivity analysis based on the Garson algorithm was conducted to quantify the effect of drying temperature and time on predicted moisture content. The analysis revealed that temperature had a dominant influence (normalized sensitivity coefficient = 0.72), while time contributed less (0.28). This indicates that temperature changes have a stronger nonlinear effect on moisture removal within the ANN framework.

Comparison between ANN and Classical Thin-Layer Models

The ANN model, being purely data-driven, can capture such nonlinearities and parameter interactions without relying on simplified assumptions. At higher drying temperatures (120 to 135 °C), both ANN and the best-performing semi-empirical models (Page and Henderson–Pabis) produced comparable accuracy, whereas at lower temperature (105 °C), ANN performed better due to its flexibility.

It should be noted that classical thin-layer models (*e.g.*, Page, Henderson–Pabis, and Logarithmic) provide echanistic or semi-empirical insights into drying kinetics, but their accuracy decreases under conditions where the drying curve deviates from simple exponential behavior. The ANN model, by contrast, is a purely data-driven approach, capable of capturing complex nonlinearities in drying behavior without requiring predefined equations. A comparative interpretation has been contributed by this work, showing that ANN predictions aligned well with the best-performing thin-layer models at higher temperatures, while outperforming them at lower temperature (105 °C), where model inadequacy was observed. Finally, the ANN approach complements traditional models, as it provides high predictive accuracy, whereas classical models remain useful for mechanistic interpretation.

Limitations of the Study

This research was conducted using a laboratory-scale halogen moisture analyzer (MB45, OHAUS), which, despite offering precise temperature control and rapid moisture measurement, presents inherent limitations when extrapolating the results to industrial drying systems. The halogen dryer operates within a small, enclosed chamber that provides uniform but static heat transfer conditions, which do not fully reflect the dynamic convective heat and mass transfer processes occurring in industrial dryers. In addition, air velocity, humidity, and fiber bed thickness were maintained constant throughout the experiments, thereby limiting the ability to analyze their combined effects on drying kinetics. The restricted sample size and localized heating zone may also lead to thermal gradients and non-uniform internal moisture diffusion, differing from large-scale drying behavior.

Moreover, the predictive performance of the artificial neural network (ANN) model is highly dependent on the size, variability, and representativeness of the experimental dataset; its accuracy may decline when applied to untested conditions. Consequently, scaling up these results requires pilot- or industrial-scale studies that account for variable airflow, humidity, and material loading. Future research should also investigate hybrid or physics-informed ANN models that combine data-driven learning with mechanistic understanding to enhance both accuracy and interpretability.

CONCLUSIONS

Several investigators have proposed over 100 different semi-theoretical and empirical thin-layer drying models for agricultural products, highlighting the complexity and variety in modeling approaches. In this study, the drying kinetics of wood fibers were evaluated using 18 semi-empirical models and an artificial neural net (ANN) model to identify the simplest model for predicting moisture changes during the drying process. The performance of the thin-layer drying models was assessed based on statistical parameters, including R^2, sum of the square of errors (SSE), and root mean squared error (RMSE). The results can be summarized as follows:

1. Among the evaluated models, the Henderson and Pabis, and Page models, each with two adjustable parameters (a, k; and k, n, respectively), provided a good and acceptable fit for the drying kinetics of wood fibers at temperatures ranging from 120 to 135 °C.
2. The ANN model did not outperform traditional thin-layer drying methods in predicting changes in moisture content, suggesting that simpler methods are often more effective.

ACKNOWLEDGEMENTS

The authors are grateful for financial support from the University of Zabol Grant Number (PR-UOZ1400-12).

REFERENCES CITED

Ademiluyi, T., Oboho, E. O., and Owudogu, M. (2008). "Investigation into the thin layer drying models of Nigerian popcorn varieties," *Leonardo Electronic Journal of Practices and Technologies* 7(13), 47-62.

Arabi, M., Faezipour, M. M., Layeghi, M., Khanali, M., and Zareahosseinabadi, H. (2017). "Evaluation of thin-layer models for describing drying kinetics of poplar wood particles in a fluidized bed dryer," *Particulate Science and Technology* 35(6), 723-730. https://doi.org/10.1080/02726351.2016.1196275

ASTM D6980-12 (2012). "Standard test method for determination of moisture in plastics by loss in weight," ASTM International, West Conshohocken, PA, USA.

Autengruber, M., Lukacevic, M., and Füssl, J. (2020). "Finite-element-based moisture transport model for wood including free water above the fiber saturation point," *International Journal of Heat and Mass Transfer* 161, article 120228. https://doi.org/10.1016/j.ijheatmasstransfer.2020.120228

Babalis, S. J., Papanicolaou, E., Kyriakis, N., and Belessiotis, V. G. (2006). "Evaluation of thin-layer drying models for describing drying kinetics of figs (*Ficus carica*)," *Journal of Food Engineering* 75(2), 205-214. https://doi.org/10.1016/j.jfoodeng.2005.04.008

Brys, A., Kaleta, A., Górnicki, K., Głowacki, S., Tulej, W., Bryś, J., and Wichowski, P. (2021). "Some aspects of the modelling of thin-layer drying of sawdust," *Energies* 14(3), article 726. https://doi.org/10.3390/en14030726

Chai, H., Chen, X., Cai, Y., and Zhao, J. (2018). "Artificial neural network modeling for predicting wood moisture content in high frequency vacuum drying process," *Forests* 10(1), article 16. https://doi.org/10.3390/f10010016

Chanpet, M., Rakmak, N., Matan, N., and Siripatana, C. (2020). "Effect of air velocity, temperature, and relative humidity on drying kinetics of rubberwood," *Heliyon* 6(10). https://doi.org/10.1016/j.heliyon.2020.e05151

Dash, K. K., Chakraborty, S., and Singh, Y. R. (2020). "Modeling of microwave vacuum drying kinetics of Bael (*Aegle marmelos* L.) pulp by using artificial neural network," *Journal of the Institution of Engineers (India): Series A* 101, 343-351. https://doi.org/10.1007/s40030-020-00431-x

Demir, V. E. D. A. T., Gunhan, T. U. N. C. A. Y., and Yagcioglu, A. K. (2007). "Mathematical modelling of convection drying of green table olives," *Biosystems Engineering* 98(1), 47-53. https://doi.org/10.1016/j.biosystemseng .2007.06.011

Dincer, I. (1998). "Moisture loss from wood products during drying—Part I: Moisture diffusivities and moisture transfer coefficients," *Energy Sources* 20(1), 67-75. https://doi.org/10.1080/ 00908 319808970044

Doymaz, I. (2007). "Air-drying characteristics of tomatoes," *Journal of Food Engineering* 78(4), 1291-1297. https://doi.org/10.1016/j.jfoodeng.2005.12.047

Fernando, N., Narayana, M., and Wickramaarachchi, W. A. M. K. P. (2018). "The effects of air velocity, temperature and particle size on low-temperature bed drying of wood chips," *Biomass Conversion and Biorefinery* 8(1), 211-223. https://doi.org/10.1007/s13399-017-0257-7

Gan, P. L., and Poh, P. E. (2014). "Investigation on the effect of shapes on the drying kinetics and sensory evaluation study of dried jackfruit," *International Journal of Science and Engineering* 7(2), 193-198. https://doi.org/10.12777/ijse.7.2.193-198

Ghazanfari, A., Emami, S., Tabil, L. G., and Panigrahi, S. (2006). "Thin-layer drying of flax fiber: II. Modeling drying process using semi-theoretical and empirical models," *Drying Technology* 24(12) 1637-1642. https://doi.org/10.1080/07373930601031463

Górnicki, K., Kaleta, A., Bryś, A., and Winiczenko, R. (2016). "Thin-layer drying of sawdust mixture," *Polish Journal of Chemical Technology* 18(4), 65-70. https://doi.org/10.1515/pjct-2016-0072

Hii, C. L., Law, C. L., and Cloke, M. (2009). "Modeling using a new thin layer drying model and product quality of cocoa," *Journal of Food Engineering* 90(2), 191-198. https://doi.org/10.1016/j.jfoodeng. 2008.06.022

Huang, D., Yang, P., Tang, X., Luo, L., and Sunden, B. (2021). "Application of infrared radiation in the drying of food products," *Trends in Food Science and Technology* 110, 765-777. https://doi.org/10.1016/j.tifs.2021.02.039

Jatmiko, T. H., Rosyida, V. T., Indrianingsih, A. W., and Apriyana, W. (2017). "Thin layer drying model of bacterial cellulose film," in: *IOP Conference Series: Earth and Environmental Science* 101(1), article 012011. https://doi.org/10.1088/1755-1315/101/1/012011

Kaleta, A., and Górnicki, K. (2010). "Evaluation of drying models of apple (var. McIntosh) dried in a convective dryer," *International Journal of Food Science & Technology* 45(5), 891-898. https://doi.org/10.1111/j.1365-2621.2010.02230.x

Kaleta, A., Górnicki, K., Winiczenko, R., and Chojnacka, A. (2013). "Evaluation of drying models of apple (var. Ligol) dried in a fluidized bed dryer," *Energy*

Conversion and Management 67, 179-185. https://doi.org/10.1016/j .enconman.2012.11.011

Kaur, K., and Singh, A. K. (2014). "Drying kinetics and quality characteristics of beetroot slices under hot air followed by microwave finish drying," *African Journal of Agricultural Research* 9(12), 1036-1044. https://doi.org/10.5897 /AJAR2013.7759

Kong, L., Yang, X., Hou, Z., and Dong, J. (2022). "Evaluation of thin-layer models for kinetic analysis in unbleached kraft pulpboard drying," *Iranian Journal of Chemistry and Chemical Engineering* 41(3), 1022-1033. https://doi.org/1021-9986/2022/3/1022-1033

Kong, L., Yang, X., Hou, Z., and Dong, J. (2020). "Mathematical modeling of drying kinetics for pulp sheet based on Fick's second law of diffusion," *Journal of Korea TAPPI* 52(2), 23-31. https://doi.org/10.7584/JKTAPPI.2020.04.52.2.23

Kumar, N., Sarkar, B. C., and Sharma, H. K. (2012). "Mathematical modelling of thin layer hot air drying of carrot pomace," *Journal of Food Science and Technology* 49, 33-41. https://doi.org/10.1007/s13197-011-0266-7

Lee, J. H., and Kim, H. J. (2009). "Vacuum drying kinetics of Asian white radish (*Raphanus sativus* L.) slices," *LWT-Food Science and Technology* 42(1), 180-186. https://doi.org/10.1016/j.lwt.2008. 05.017

Li, X., and Zhao, Z. (2020). "Time domain-NMR studies of average pore size of wood cell walls during drying and moisture adsorption," *Wood Science and Technology* 54(5), 1241-1251. https://doi.org/10.1007/s00226-020-01209-x

Midilli, A. D. N. A. N., Kucuk, H. A. Y. D. A. R., and Yapar, Z. İ. Y. A. (2002). "A new model for single-layer drying," *Drying technology* 20(7), 1503-1513. https://doi.org/10.1081/DRT-120005864

Penttila, P. A., Paajanen, A., and Ketoja, J. A. (2021). "Combining scattering analysis and atomistic simulation of wood-water interactions," *Carbohydrate Polymers* 251, article 117064. https://doi.org/10.1016/j.carbpol.2020.117064

Remond, R., Perré, P., and Mougel, E. (2005). "Using the concept of thin dry layer to explain the evolution of thickness, temperature, and moisture content during convective drying of Norway spruce boards," *Drying Technology* 23(1-2), 249-271. https://doi.org/10.1081/DRT-200047883

Salin, J. G. (2008). "Drying of liquid water in wood as influenced by the capillary fiber network," *Drying Technology* 26(5), 560-567. https://doi.org/10.1080/07373930801944747

Sander, A., Kardum, J. P., & Glasnović, A. (2010). "Drying of solids; estimation of the mathematical model parameters," *The Canadian Journal of Chemical Engineering*, 88(5), 822-829.

Saxena, G., Gaur, M. K., and Kushwah, A. (2022). "Performance analysis and ANN modelling of apple drying in ETSC-assisted hybrid active dryer," in: *Artificial Intelligence and Sustainable Computing: Proceedings of ICSISCET* 2020, pp. 275-294. https://doi.org/10.1007/978-981-16-1220-6_24

Sjöstrand, B., Karlsson, C.-A., Barbier, C., and Henriksson, G. (2023). "Hornification in commercial chemical pulps: Dependence on water removal and hornification mechanisms," *BioResources* 18(2), 3856-3869. https://doi.org/10.15376/biores.18.2.3856-3869

Vega, A., Fito, P., Andrés, A., and Lemus, R. (2007). "Mathematical modeling of hot-air drying kinetics of red bell pepper (var. Lamuyo)," *Journal of food Engineering* 79(4), 1460-1466. https://doi.org/10.1016/j.jfoodeng.2006.04.028

Verma, L. R., Bucklin, R. A., Endan, J. B., and Wratten, F. T. (1985). "Effects of drying air parameters on rice drying models," *Transactions of the ASAE* 28(1), 296-0301.

Wang, C. Y., and Singh, R. P. (1978). "A single layer drying equation for rough rice," *ASAE paper* No. 78-3001, MI, USA.

Wang, Z., Sun, J., Liao, X., Chen, F., Zhao, G., Wu, J., and Hu, X. (2007a). "Mathematical modeling on hot air drying of thin layer apple pomace," *Food Research International*, 40:39–46.

Wang, S., Zhang, Y. and Xing, C. (2007). "Effect of drying method on the surface wettability of wood strands," *Holz Roh Werkst* 65, 437-442. https://doi.org/10.1007/s00107-007-0191-7

Wiberg, P., and Morén, T. J. (1999). "Moisture flux determination in wood during drying above fiber saturation point using CT-scanning and digital image processing," *Holz als Roh-und Werkstoff* 57(2), 137-144. https://doi.org/10.1007/s001070050029

Younis, M., Abdelkarim, D., and El-Abdein, A. Z. (2018). "Kinetics and mathematical modeling of infrared thin-layer drying of garlic slices," *Saudi Journal of Biological Sciences* 25(2), 332-338. https://doi.org/10.1016/j.sjbs.2017.06.011

Zarea Hosseinabadi, H., Doosthoseini, K., and Layeghi, M. (2012). "Kinetika konvektivnog sušenja tankog sloja iverja drva topole (*Populus deltoides*)," *Drvna Industrija* 63(3), 169-176. https://doi.org/10.5552/drind.2012.1201

Zitting, A., Paajanen, A., Rautkari, L., and Penttilä, P. A. (2021). "Deswelling of microfibril bundles in drying wood studied by small-angle neutron scattering and molecular dynamics," *Cellulose* 28, 10765-10776. https://doi.org/10.1007/s10570-021-04204-y

Article submitted: February 13, 2025; Peer review completed: April 5, 2025; Revised version received: October 13, 2025; Further revised version received and accepted: November 15, 2025; Published: December 3, 2025.
DOI: 10.15376/biores.21.1.654-672